Advanced Composites and Hybrid Materials (2023) 6:42
https://doi.org/10.1007/s42114-022-00605-0

ORIGINAL RESEARCH

Top-down digital light processing 3D printing of composite structures using carbon fiber modified UV curable resin

Crystal Lu[1] · Kaiyue Deng[2] · Annie Porter[2] · Kun (Kelvin) Fu[2,3]

Received: 22 April 2022 / Revised: 31 October 2022 / Accepted: 14 December 2022 / Published online: 13 January 2023

Abstract

Utilizing the shear-thinning property of carbon-fiber modified resins, composite structures were fabricated by digital light processing (DLP) 3D printing. The rheological behaviors of the resins were studied with different loading ratios of carbon fibers. Curing kinetics of the resins were analyzed using Fourier transform infrared spectroscopy–attenuated total reflectance (FTIR-ATR). The effects of different carbon fiber loading ratios on the mechanical and thermal properties of the fabricated structures were investigated by tensile testing and thermal gravimetric analysis (TGA). It was found that the Young's modulus and tensile strength first showed a monotonic increase with an increasing carbon-fiber loading ratio up to 7.5%. However, when the loading ratio was further increased to 10.0%, the mechanical strengths of the fabricated parts decreased. Specifically, with a 7.5% weight percentage of carbon fibers in the resin, an improvement factor of 536% in Young's modulus and 323% in ultimate tensile strength was obtained in the resultant 3D printed parts. Additionally, the weight loss analyzed by TGA suggested that incorporating carbon fibers in the UV curable resin can help enhance the thermal stability of the fabricated parts. Models made of unmodified resin and carbon fiber-modified resin were tested for vulcanizing applications, in which the 3D printed models were embedded in rubber to form shape-complementary cavities under high temperature and high pressure. Casting pieces resulting from the models printed with carbon fiber–modified resin showed dramatically improved surface quality. The improvement in the casting performance was attributed to the enhancement in the thermal and mechanical properties caused by the addition of carbon fibers.

Keywords Digital light processing · 3D printing · Carbon fiber · Photopolymer resin · Mechanical strength

1 Introduction

Advanced composites and hybrid materials have potential applications in many industrial sectors, spanning from aerospace, automotive and energy to novel electronics, medical devices, and sensors [1]. By combining different components, the resultant materials demonstrate superior electrical [2], thermal [3], and mechanical [4] properties than their constituents. With the advent of 3D printing, complex structures can be directly manufactured without the need for conventional tooling, thus enabling substantial time and cost savings [5, 6]. Recently, there has been abundant research geared toward fabricating composites and hybrid materials using filament- [7, 8] and ink-based 3D printing techniques [9–12]. By incorporating different fillers in thermoplastic filaments or photocurable resins, 3D models can be fabricated using fused deposition modeling (FDM) or digital light processing (DLP) printers, respectively. Because carbon fiber is a material with one of the highest strength-to-weight ratios, it has been widely used as a filler to enhance material strength. Specifically, carbon fibers have been added to thermoplastic filaments used in FDM-based 3D printing [13]. More than 20.0% increases in Young's modulus and tensile strength have been demonstrated with the resultant 3D printed composite. It may appear straightforward that adding carbon fiber into the photocurable resin can lead to similar mechanical property improvement. Additionally, compared to its FDM counterpart, the DLP 3D printing enables a much shorter fabrication time because each layer

✉ Kun (Kelvin) Fu
kfu@udel.edu

[1] Charter School of Wilmington, 100 N Dupont Rd, Wilmington, DE 19807, USA

[2] Department of Mechanical Engineering, University of Delaware, Newark, DE 19716, USA

[3] Center for Composite Materials, University of Delaware, Newark, DE 19716, USA

of a 3D model is simultaneously cured, while FDM employs line-by-line raster scans. Furthermore, the spatial resolution of DLP printing is generally better than that of FDM (i.e., tens vs. hundreds of microns). However, DLP 3D printing of carbon composites has the following challenges: (1) it may be difficult for the carbon fibers to be well dispersed and remain suspended in the resin during the printing process [14]; (2) a high loading ratio of carbon fibers may be needed to achieve the desired property enhancements, but it may cause printing issues due to the high viscosity and low UV penetration depth of the resultant resin [15]; (3) desired 3D network of carbon fibers in the photopolymer matrix [16] may be difficult to form with common bottom-up DLP printing methods, in which a layer of resin is squished between the printing platform and the resin container, thus compromising the fiber alignment and strength enhancement along the printing direction; and (4) optimal fiber length [17] for mechanical property enhancement may be incompatible with DLP printing. It was previously found that there existed an optimal length [17] to achieve the mechanical strength enhancement by carbon fibers in FDM filaments. Fibers with such optimal lengths can provide mechanical strength enhancement but may be too long for good resolutions in the resultant parts when DLP 3D printing is used instead.

A top-down DLP printer was used to fabricate the testing samples used in this study. Figure 1a illustrates the top-down printing process: a sample build platform was immersed in the resin by a predetermined depth/layer resolution (i.e., 50 μm). The cross-sectional image of a model was projected onto the resin by a DLP projector. After a layer was cured, the projection pattern was switched to a blank screen, and the build stage was lowered into the resin. A settling time was used to ensure that the resin flowed from the neighboring area to cover the previously cured layer. The cross-sectional image for the next layer was subsequently projected onto the resin. Consequently, a complete 3D model could be printed after many iterations. Figure 1b shows the model used for fabricating the type V tensile testing samples according to ASTM D638-14 standard. Raft and supports were added to obtain improved build plate adhesion and easy model removal after printing. Such a model was constructed and sliced using Chitubox software to generate the projection patterns. All testing specimens were printed using 100 raft layers and a support height of 5 mm. The layer resolution was 0.05 mm and the bottom raft layer was cured for 20 s. Because the number of free radicals that can be generated is proportional to the cross-sectional areas of the patterns, smaller areas require longer curing times. Therefore, the exposure times for the support and normal layers (i.e., the dog bone model) were 12 s and 3 s, respectively, for all the resins. A settling time of 4 s in the resin was used for all samples.

It should be noted that the top-down printer is different from its bottom-up counterparts. In commercial bottom-up DLP printers, the resin is flushed into the area between the build plate and the resin container, and is pressed against the vat during UV exposure. After a layer is printed, the cured portion is then peeled from the vat film and lifted above the resin level. Such frequent peeling actions can cause the printed model to detach from the build plate, particularly for viscous resin. Additionally, constant pressing against the vat film may also lead to fiber alignment along the plane direction, thus preventing the formation of 3D network structures to achieve the desired mechanical strength enhancement.

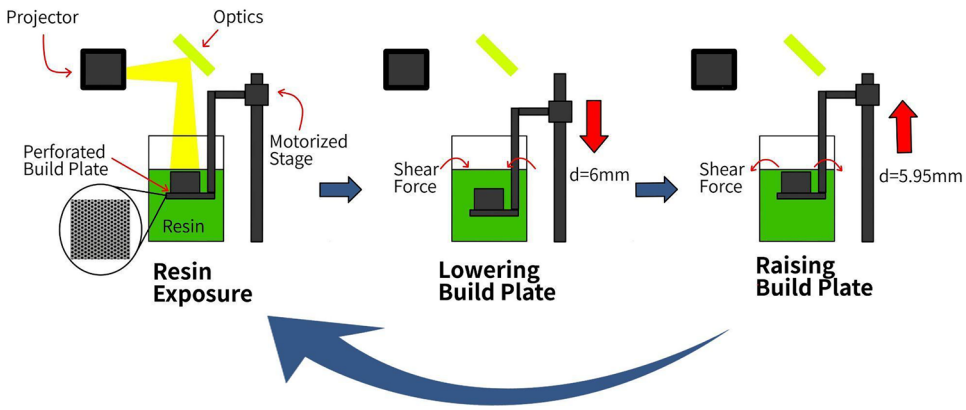

Fig. 1 Illustration of the top-down DLP 3D printing process. Schematic of the 3D printing process. The build plate was first brought to the home position so that it was flush with the resin surface. After the cross-sectional images of a 3D model were obtained using a slicing software, they were sequentially projected onto the resin surface using a DLP projector. A layer was fabricated after light exposure. The projection pattern was then switched to a blank screen and the build plate was then quickly lowered beneath the resin surface by a predetermined distance (e.g., 6 mm). A settling time was used to allow the resin to flow and cover the previously printed layer. The build plate was then quickly raised by another distance (i.e., 6 mm—desired layer thickness). After another settling time, the pattern of the next layer is then projected onto the resin to start another exposure cycle. A complete model can be printed layer by layer after many iterations

These problems, however, are eliminated by using the current top-down DLP printer. It should also be emphasized that the current top-down DLP printer is better suited for 3D printing with viscous resins. Because most resin materials have shear-thinning characteristics, by quickly lowering/raising the build plate with a speed of 250 mm/min, which is about 4 times faster than the conventional lifting speed, the generated shear force can reduce the resin viscosity to allow better surface recoating and self-leveling.

2 Results and discussions

Figure 2a shows a picture of the resin with and without the carbon fiber. The carbon fibers were thoroughly mixed into the resin using the high shear mixer and remained suspended several hours after mixing. Because the settling time for the carbon fibers in the resin was much longer than the printing time, no agitation was used during the printing process. The viscosity as a function of the shear rate is shown in Fig. 2b. All the resin samples showed shear thinning characteristics: the measured viscosity decreased with an increasing shear rate. Such a shear-thinning property can be utilized by the aforementioned top-down DLP printing process: by quickly lowering and raising the build platform, the resultant shear stress can temporarily reduce the resin viscosity to allow good layer re-coating. It should be noted that the starting material (i.e., the pure resin) showed relatively low viscosity (i.e., ~ 100 mPa·s at a shear rate of 10 s^{-1}). The viscosity of the resin increased sharply with an increasing loading ratio of the carbon fibers, and it reached high values when the mixed carbon fibers were above 10.0% (i.e., 2.8 and 4.5 Pa·s at a shear rate of 10 s^{-1} for resins containing 10.0% and 15.0% carbon fibers, respectively). Figure 2c shows representative pictures of the dog bone testing samples printed using the original and carbon fiber modified resin. Models were successfully printed using resin containing up to a weight percentage of 10.0% carbon fibers. Attempts were made to print models using resin containing 15.0% carbon fiber, but they were unsuccessful even with extended layer exposure time (e.g., 20 s). More carbon fibers in the resin can lead to decreased effective photo-initiator concentration, higher viscosity, and lower UV light penetration depth. Consequently, it is difficult for the resin containing more than 10.0% carbon fibers to flow, evenly cover previously printed layers, and become fully cured even with extended curing time. Instead of a solid and uniformly cured part, a sponge-like structure consisting of uncured resin sandwiched between cured thin layers was observed. Previously, it was found that the resin viscosity should not exceed 3 Pa·s to be compatible with commercial DLP printers and to achieve a good layer recoating and self-leveling [18]. The current results appeared to be in good agreement with those requirements. Nevertheless, parts printed using resin containing up

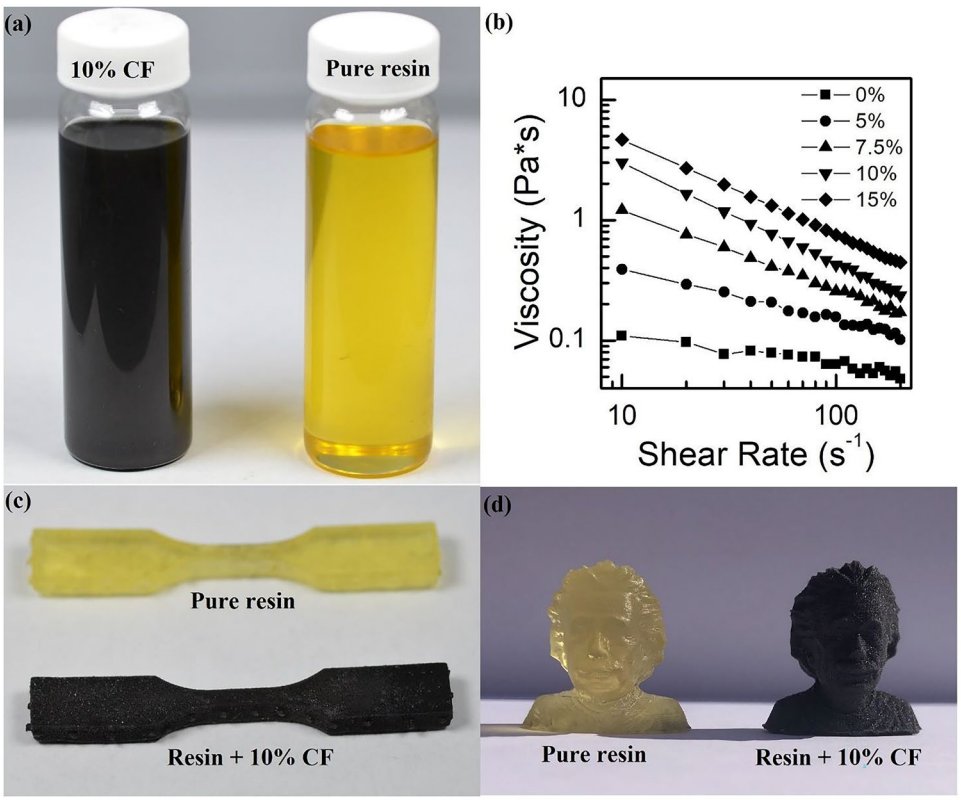

Fig. 2 Digital photos and measured viscosity of the resins used for printing, and printed samples. **a** Picture of the original and carbon fiber-modified resin. **b** Viscosity as a function of the shear rate measured from resin samples containing different weight percentages of carbon fibers. **c** Picture of the type V dog bone testing samples. **d** Picture of the printed human head sculptures

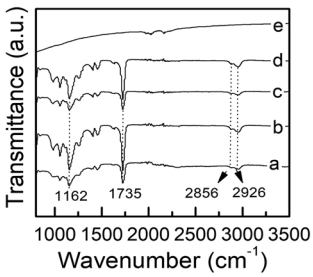

Fig. 3 FTIR spectra measured from printed samples and carbon fibers. **a** Sample printed with pure resin. **b** Sample printed from resin containing 5.0% carbon fiber. **c** Sample printed from resin containing 7.5% carbon fiber. **d** Sample printed from resin containing 10.0% carbon fiber. **e** Pure carbon fibers

to 10.0% carbon fibers showed very good printing quality. Figure 2d shows sample 3D prints using the original and 10.0 wt% carbon fiber modified resin. All features of the original 3D model were successfully transferred to the 3D prints and their qualities are similar.

FTIR spectra of samples printed with resin containing carbon fibers suggest that they are composites in nature. Unlike hybrid materials where new spectral features are often introduced by fillers, the resultant composites showed virtually the same absorptive bands as the sample printed with pure resin. As shown in Fig. 3, all samples showed absorptive features that are representative of acrylate polymers [19]. Specifically, the bands at 1735 cm^{-1} and 1162 cm^{-1} correspond to C=O stretching vibration and C–O stretching of the ester group, while those at 2926 cm^{-1} and 2856 cm^{-1} are assigned to stretching vibration of –CH3 and –CH2, respectively.

Figure 4a shows the stress–strain curves of the dog bone testing samples printed with resin containing different weight percentages of carbon fibers. The curves for all samples showed brittle characteristics: no strain hardening was observed, and the parts fractured instantaneously at the ultimate tensile strength. Samples printed using carbon fiber-modified resins showed significantly higher Young's moduli and ultimate tensile strength as shown in Fig. 4b, c. Specifically, the Young's moduli are 0.20 GPa, 0.61 GPa, 1.25 GPa, and 1.18 GPa and tensile strengths are 16.25 MPa, 34.61 MPa, 61.97 MPa, and 57.18 MPa for samples printed using resins containing 0%, 5.0%, 7.5%, and 10.0% carbon fibers, respectively. Samples printed using resin containing

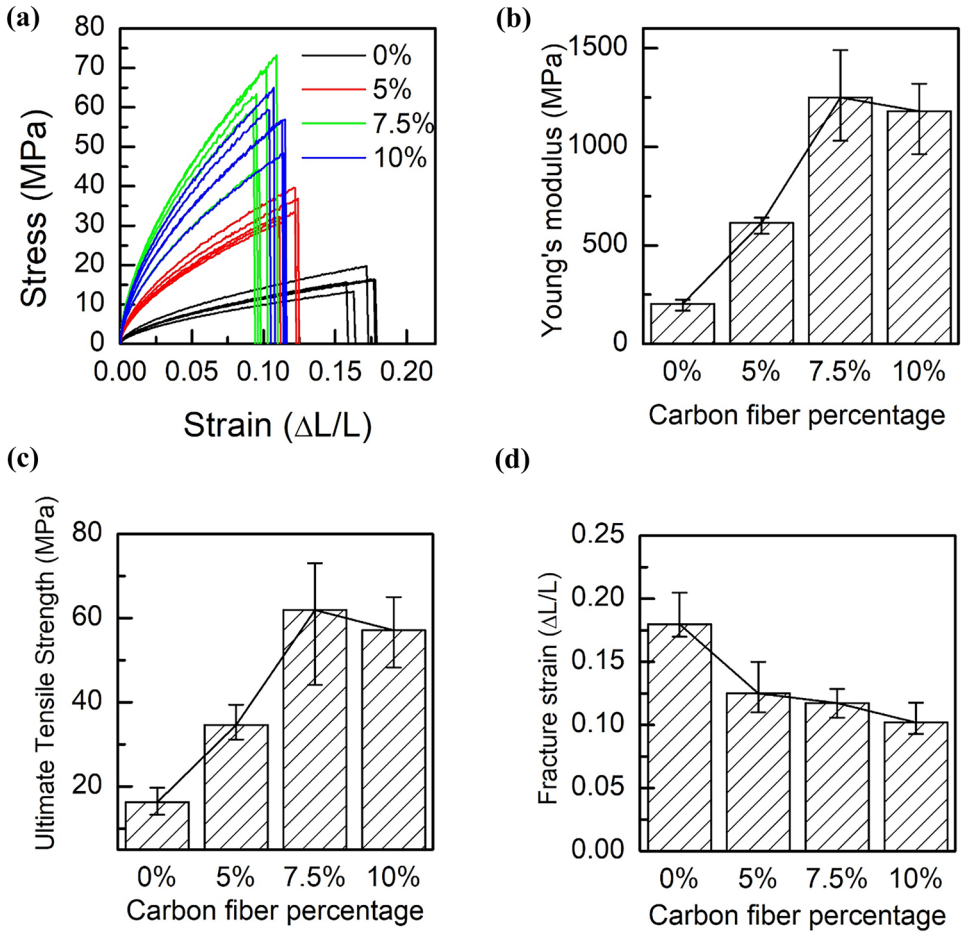

Fig. 4 Mechanical testing results of the 3D-printed dog bone samples using resins containing 0%, 5.0%, 7.5%, and 10.0% carbon fibers. **a** Results of stress–strain curves. **b** Results of Young's modulus. **c** Results of ultimate tensile strength. **d** Results of fracture strain

7.5% carbon fibers demonstrated the highest Young's modulus (1.25 GPa) and ultimate tensile strength (61.97 MPa). Compared to the samples fabricated using unmodified resin, improvement factors of 536% and 323% were obtained, respectively. It should be noted that Young's modulus and ultimate tensile strength did not increase with an increasing percentage of carbon fiber in the resin. Instead, these mechanical properties peaked at 7.5% and then decreased with more carbon fibers in the resin. The decreases in mechanical properties at a higher carbon fiber loading ratio were attributed to the insufficiently cured interfaces. With increasing carbon fibers in the resin, both the effective photoinitiator concentration and light penetration depth decreased, leading to poor interface adhesion even with increased layer exposure time. The fracture strain, however, showed a monotonic decrease with an increasing weight percentage of carbon fiber in the resin. Figure 4d shows that the averaged fracture strains are 0.180, 0.125, 0.118, and 0.102 for samples printed using 0%, 5.0%, 7.5%, and 10.0% carbon fiber modified resins, respectively.

Figure 5a shows the TGA curves for the samples printed using resin containing different amounts of carbon fibers. All the samples showed rapid weight losses at temperatures in the range of 300 to 500 °C, which corresponded to polymer decomposition into gaseous monomers and mixtures of low molecular weight alcohols [20]. Across the entire temperature range, the order of weight loss alternated: in the low- to intermediate-temperature range (i.e., < 300 °C), samples printed with pure resin and 5.0 wt% carbon fibers showed the lowest weight loss, while those printed with 7.5 wt% and 10.0 wt% carbon fibers had the highest weight loss. Such a trend changed in the temperature range from 300 to 375 °C, at which samples printed with resin containing 10.0 wt% carbon fibers showed the lowest weight loss, while those fabricated with pure resin showed highest weight loss. At the temperature above 600 °C, all the polymer matrices were completely decomposed such that only the carbon fibers remained. The retained weight percentages agreed well with the loading ratios of carbon fibers in the resin of those samples. Figure 5b shows the weight percentage at low to intermediate temperatures. The thermal decompositions in acrylic polymers are rather complex processes. While depolymerization reactions are the major decomposition mechanism at high temperatures, the chain scission reactions are generally responsible in the low- to intermediate-temperature range [21]. The incorporation of carbon fibers in the acrylic polymer matrix may affect both reaction mechanisms, thus leading to different thermal decomposition behaviors. Additionally, carbon fibers in the polymer matrix may affect the extent of carbonaceous char formation, which could provide resistance to heat transfer to the unreacted polymer and reduce the flux of fuel to the vapor phase in a fire [22]. Furthermore, the dispersion quality differences among resins containing different carbon fibers may also play an important role in the thermal decomposition behaviors of the resultant polymer composites. Nevertheless, it appears beneficial to add an optimum amount of carbon fibers in the resin to achieve parts with enhanced thermal stability, although such an optimum amount may differ for applications in different temperature ranges.

Figure 6a summarizes the absorptive features of pure resin when it was subjected to UV illumination for different durations. Major absorption peaks were observed in the following ranges: 1400–1420 cm^{-1}, 1600–1650 cm^{-1}, and 1700–1750 cm^{-1} and they corresponded to the C = C twisting, stretching, and C = O stretching in the acrylate monomers, respectively [23–25]. The former two features decreased with an increasing UV exposure time, while the latter feature remained virtually unchanged. Previously, the areas under such absorptive features have been utilized to calculate the degree of conversion in acrylate ester monomer-based ceramic suspension and good agreements have

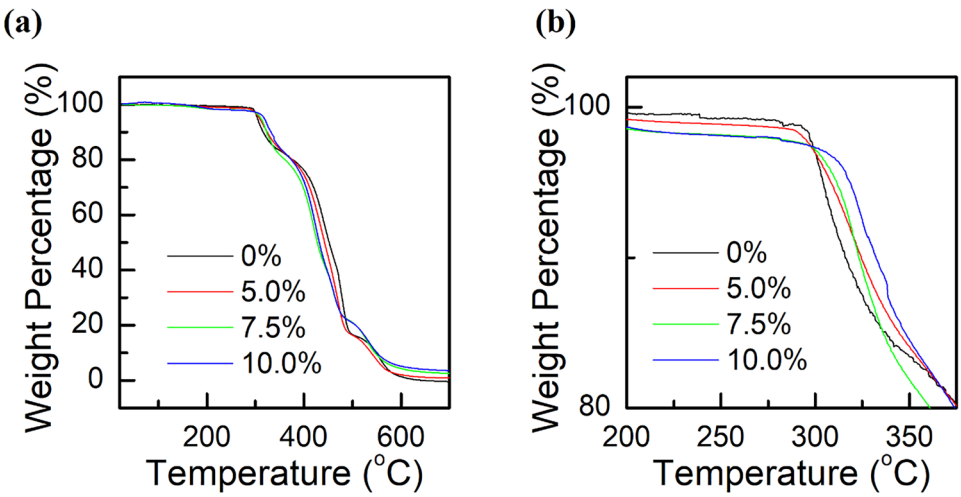

Fig. 5 TGA results of the samples printed with resin containing 0%, 5.0%, 7.5%, and 10.0% carbon fibers. **a** TGA results within the full temperature (25 to 700 °C). **b** TGA results within the intermediate temperature range from 200 to 375 °C

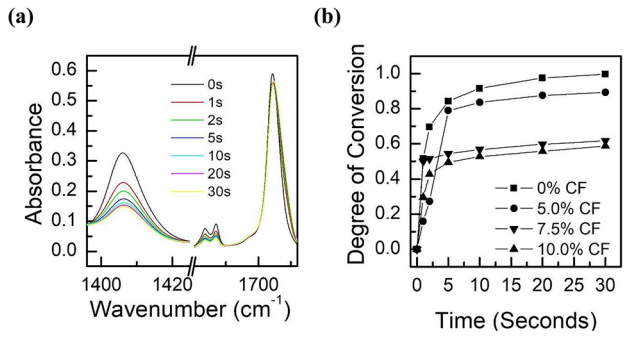

Fig. 6 Curing kinetics of the resin measured using FTIR-ATR setup. **a** Absorption spectra of the pure resin under UV illumination for different durations ranging from 0 to 30 s. **b** calculated degree of conversion for resins containing different concentrations of carbon fibers based on the absorptive features

been achieved between the results obtained using FTIR and photo-DSC [26]. Similarly, such an approach is adopted here and the degree of conversion in resins containing different carbon fibers was extracted and the results are summarized in Fig. 6b. A relatively high degree of conversion (i.e., > 90%) was observed in the pure resin and the one containing 5% carbon fibers. For the resin containing a higher weight percentage of carbon fibers, however, the degree of conversion was significantly lower (i.e., ~ 60%) even at extended UV exposure time of 30 s. Resin containing 7.5% and 10.0% carbon fiber showed similar curing behavior. The curing kinetics in the free-radical polymerization system is rather complex: the curing processes involve photodecomposition, photoinitiation, propagation, and chain transfer reactions and termination [27]. A larger carbon fiber loading ratio leads to decreased photoinitiator content and UV penetration depth but increased viscosity, thus affecting the photodecomposition, photoinitiation, and propagation steps. Additionally, the incorporation of carbon fibers may also affect the chain length and flexibility of the macro-radicals involved in the termination reaction [28]. Although the UV power intensity used for the real-time FTIR measurements may be different from that of the 3D DLP printer and the light source used in the printer has much broader emission wavelengths, these results suggest that the incorporation of carbon fibers indeed changed the curing kinetics in the acrylate-based monomers. The differences in the degree of curing may lead to different thermal and mechanical properties of the resultant 3D printed parts.

Figure 7a–d shows representative SEM images for samples printed with resin containing 0%, 5.0%, 7.5%, and 10.0% carbon fibers, respectively. The morphology for all samples showed very good 3D printing quality. The cured photopolymers are dense and uniform; virtually no voids caused by trapped air bubbles were present. Additionally, the carbon fibers were evenly distributed in the photopolymer

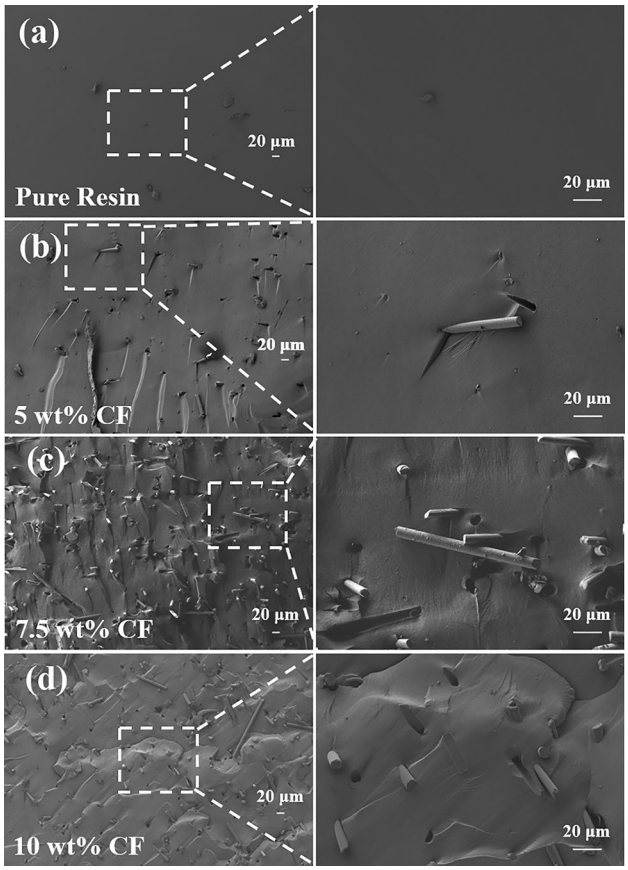

Fig. 7 Representative SEM images of the fractured surface for samples. **a** SEM images of the printed sample containing 0% carbon fibers. **b** 5.0 wt% carbon fibers, **c** 7.5 wt% carbon fibers, and **d** 10.0 wt% carbon fibers

matrix and no conglomerations were observed. Furthermore, the orientation of the carbon fibers in the samples appeared to be omnidirectional instead of being aligned parallel to the printing plane, avoiding the aforementioned drawback of the bottom-up type of 3D printers. Using the top-down DLP printers, the carbon fibers can be incorporated into the photopolymer matrix in different directions, thus resulting in a three-dimensional interconnected network. It should be emphasized that the morphology of the samples printed using the DLP resin printers was drastically better than those fabricated using the filament-based printers. In Ref. [13], the carbon fibers were generally surrounded by voids in the thermoplastic matrix. Although the mechanical properties were improved by adding carbon fibers in the printing filament, an improvement factor of only ~ 20.0% was obtained. With the current top-down DLP printers, however, much higher improvement factors of 536% and 323% for the Young's modulus and ultimate tensile strength were obtained. The significantly improved mechanical properties were attributed to the better morphology and 3D network formed by the carbon fibers.

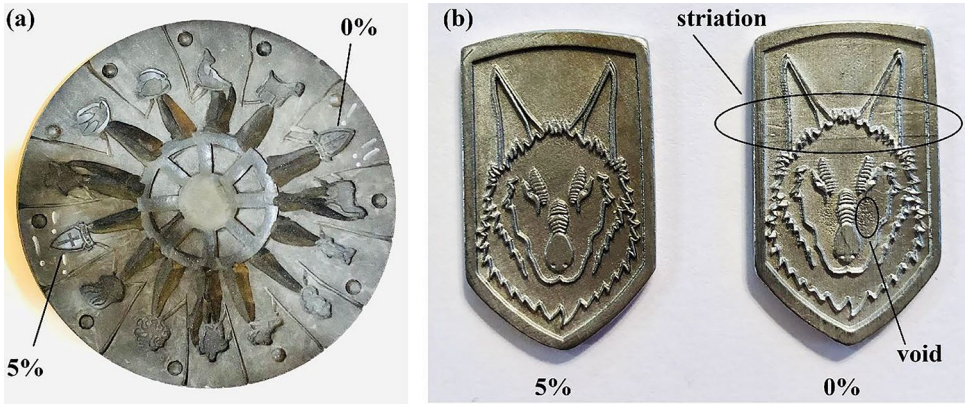

Fig. 8 Demonstration of part quality of 0% and 5.0% carbon fiber modified resin. **a** Picture of the rubber mold formed by vulcanizing processes using 3D printed parts with 0% and 5.0% carbon fiber modified resin. **b** Picture of the casting pieces resulted from 3D printed parts with 0% and 5.0% carbon fiber modified resin

Figure 8a shows the rubber mold resulted from the vulcanizing process. Compared to the mold cavities formed by 3D printed parts using pure resin, those resulting from parts printed with 5.0% carbon fibers showed consistently better quality. The surfaces were smoother, and no cracks or striations were observed. The mold surfaces resulted from pure resin, however, showed relatively dull surfaces and striations. The mold quality differences were attributed to different thermomechanical properties of the 3D printed parts. Because the parts fabricated with pure resin had lower mechanical strength and worse temperature stability, they tend to deform and crack during the vulcanization process, leading to the formation of striation and voids in certain areas. Parts printed with resin containing 5.0% carbon fibers can better stand the high-temperature and high-pressure environment during the vulcanizing processes. Figure 8b shows representative casting results. Striations and voids were observed in the piece casted from the mold resulting from pure resin. Such defects were absent from the pin casted using the mold fabricated with 5.0% carbon fiber. These results qualitatively corroborated that adding carbon fibers to the resin can help improve the mechanical and thermal properties of the 3D printed parts.

3 Conclusions

In conclusion, carbon fibers were added to acrylate-based UV curable resin and parts were successfully printed with a top-down DLP printer. High-quality 3D printed composite parts with good morphology were obtained with a carbon fiber loading ratio up to 10.0%. Mechanical tensile testing and TGA results have shown that both mechanical strengths and thermal stability of the 3D printed parts can be improved by adding carbon fibers into the photocurable resin. FTIR analysis showed that the incorporation of the carbon fibers changed the curing kinetics in the resultant photopolymer resin. Different degrees of conversion were observed and they were attributed to the effects of carbon fibers on the resin curing process involving radical generation, propagation, and chain transfer reactions and termination. Models printed using regular and carbon fiber–modified resin were subjected to vulcanizing and their performances were compared. The carbon-fiber modified resin showed consistently better mold quality and casting results, which qualitatively validated the thermal–mechanical performance improvement caused by the fibers. These results suggest that adding carbon fibers into photocurable resin is an effective method to enhance the properties of the resultant 3D printed parts. Such improved resin may enable resin-based DLP printing to be used in wider applications where high-temperature stability and good mechanical strength are critical. Although improved vulcanizing performances were demonstrated in this article, by no means the fiber-enhanced photocurable resin is limited to fabricating mold pieces for vulcanization. Potential applications may include the fabrication of mechanical connectors, adaptors, microfluidic devices, and sensors used in high-temperature, high-pressure, and corrosive environments.

Supplementary Information The online version contains supplementary material available at https://doi.org/10.1007/s42114-022-00605-0.

Declarations

Conflict of interest The authors declare no competing interests.

References

1. Gu H, Liu C, Zhu J, Gu J, Wujcik EK, Shao L, Wang N, Wei H, Scaffaro R, Zhang J, Guo Z (2018) Introducing advanced composites and hybrid materials. Adv Compos Hybrid Mater 1:1–5. https://doi.org/10.1007/s42114-017-0017-y
2. Kashfipour MA, Mehra N, Zhu J (2018) A review on the role of interface in mechanical, thermal, and electrical properties of polymer composites. Adv Compos Hybrid Mater 1:415–439. https://doi.org/10.1007/s42114-018-0022-9
3. He X, Ou D, Wu S, Luo Y, Ma Y, Sun J (2022) A mini review on factors affecting network in thermally enhanced polymer

composites: filler content, shape, size, and tailoring methods. Adv Compos Hybrid Mater 5:21–38. https://doi.org/10.1007/s42114-021-00321-1
4. Gu H, Ma C, Liang C, Meng X, Gu J, Guo Z (2017) A low loading of grafted thermoplastic polystyrene strengthens and toughens transparent epoxy composites. J Mater Chem C 5:4275–4285. https://doi.org/10.1039/C7TC00437K
5. Wickramasinghe S, Do T, Tran P (2020) FDM-based 3D printing of polymer and associated composite: a review on mechanical properties, defects and treatments. Polymers 12:1529–1570. https://doi.org/10.3390/polym12071529
6. Chen SG, Yang J, Jia YG, Lu B, Ren L (2019) TiO_2 and PEEK reinforced 3D printing PMMA composite resin for dental denture base applications. Nanomaterials 9(7):1049–1066. https://doi.org/10.3390/nano9071049
7. Mei H, Ali Z, Ali I, Cheng L (2019) Tailoring strength and modulus by 3D printing different continuous fibers and filled structures into composites. Adv Compos Hybrid Mater 2:312–319. https://doi.org/10.1007/s42114-019-00087-7
8. Wang B, Zhang Z, Pei Z, Qiu J, Wang S (2020) Current progress on the 3D printing of thermosets. Adv Compos Hybrid Mater 3:462–472. https://doi.org/10.1007/s42114-020-00183-z
9. Desai PD, Jagtap RN (2021) Synthesis and characterization of fiber-reinforced resorcinol epoxy acrylate applied to stereolithography 3D printing. ACS Omega 6(46):31122–31131. https://doi.org/10.1021/acsomega.1c04566
10. Xiao T, Qian C, Yin R, Wang K, Gao Y, Xuan F (2020) 3D printing of flexible strain sensor array based on UV-curable multiwalled carbon nanotube/elastomer composite. Adv Mater Technol 6(1):2000745. https://doi.org/10.1002/admt.202000745
11. Feng Z, Li Y, Hao L, Yang Y, Tang T, Tang D, Xiong W (2019) Graphene-reinforced biodegradable resin composites for stereolithographic 3D printing of bone structure scaffolds. J Nanomater 2019:1–13. https://doi.org/10.1155/2019/9710264
12. Wang J, Liu Y, Fan Z, Wang W, Wang B, Guo Z (2019) Ink-based 3D printing technologies for graphene-based materials: a review. Adv Compos Hybrid Mater 2:1–33. https://doi.org/10.1007/s42114-018-0067-9
13. Ning F, Cong W, Qiu J, Wei J, Wang S (2015) Additive manufacturing of carbon fiber reinforced thermoplastic composites using fused deposition modeling. Compos B Eng 80:369–378. https://doi.org/10.1016/j.compositesb.2015.06.013
14. Jiménez-Suárez A, Campo M, Sánchez M, Romón C, Ureña A (2012) Dispersion of carbon nanofibres in a low viscosity resin by calendering process to manufacture multiscale composites by VARIM. Compos B Eng 43:3104–3113. https://doi.org/10.1016/j.compositesb.2012.04.030
15. Tu J, Makarian K, Alvarez NJ, Palmese GR (2020) Formulation of a model resin system for benchmarking processing-property relationships in high-performance photo 3D printing applications. Materials (Basel, Switzerland) 13(18):4109–4123. https://doi.org/10.3390/ma13184109
16. Bisht A, Dasgupta K, Lahiri D (2019) Investigating the role of 3D network of carbon nanofillers in improving the mechanical properties of carbon fiber epoxy laminated composite. Compos Part A Appl Sci and Manuf 126:105601. https://doi.org/10.1016/j.compositesa.2019.105601
17. Ning F, Cong W, Qiu J, Wei J, Wang S (2015) Additive manufacturing of CFRP composites using fused deposition modeling: effects of carbon fiber content and length. Proceedings of the ASME 2015 International Manufacturing Science and Engineering Conference. Volume 1: Processing. Charlotte, North Carolina, USA. https://doi.org/10.1115/MSEC2015-9436
18. Komissarenko D, Sokolov P, Evstigneeva A, Shmeleva I, Dosovitsky A (2018) Rheological and curing behavior of acrylate-based suspensions for the DLP 3D printing of complex zirconia parts. Materials 11(12):2350–2361. https://doi.org/10.3390/ma11122350
19. Yun H, Zhang X (2020) Fabrication and characterization of hexadecyl acrylate cross-linked phase change microspheres. e-Polymers 20(1):69–75. https://doi.org/10.1515/epoly-2020-0008
20. Czech Z, Agnieszka K, Ragańska P, Antosik A (2015) Thermal stability and degradation of selected poly(alkyl methacrylates) used in the polymer industry. J Therm Anal Calorim 119:1157–1161. https://doi.org/10.1007/s10973-014-4290-5
21. Johnston PK, Doyle E, Orzel RA (1988) Acrylics: a literature review of thermal decomposition products and toxicity. J Med Toxicol 7:139–200. https://doi.org/10.3109/10915818809014519
22. Erickson K (2007) Thermal decomposition of polymers in nitrogen and in air. SAND2007–5405C. Sandia National Laboratory, Albuquerque, NM, USA. https://www.osti.gov/servlets/purl/1147465. Accessed 22 Oct 2022
23. Sideridou I, Tserki V, Papanastasiou G (2002) Effect of chemical structure on degree of conversion in light-cured dimethacrylate-based dental resins. Biomaterials 23(8):1819–1829. https://doi.org/10.1016/S0142-9612(01)00308-8
24. Lin-Vien D, Colthup N, Fateley W, Grasselli J (1991) The handbook of infrared and Raman characteristic frequencies of organic molecules, 1st edn. Academic Press, San Diego, California, pp 137–281
25. Chrószcz MW, Barszczewska-Rybare I, Wori P (2021) The relationship between the degree of conversion in dental dimethacrylate polymers determined by infrared spectroscopy and polymerization shrinkage. Eng Proc 11(1):52. https://doi.org/10.3390/ASEC2021-11151
26. Wu K, Halloran J (2005) Photopolymerization monitoring of ceramic stereolithography resins by FTIR methods. J Mater Sci 40:71–76. https://doi.org/10.1007/s10853-005-5689-y
27. Goodner M, Bowman C (1999) Modeling primary radical termination and its effects on autoacceleration in photopolymerization kinetics. Macromolecules 32:6552–6559. https://doi.org/10.1021/ma9901947
28. Lang M, Hirner S, Wiesbrock F, Fuchs P (2022) A review on modeling cure kinetics and mechanisms of photopolymerization. Polymers 14:2074-2131. https://doi.org/10.3390/polym14102074